Received April 20, 2018, accepted May 22, 2018, date of publication June 4, 2018, date of current version June 26, 2018.

Digital Object Identifier 10.1109/ACCESS.2018.2843333

Transmission Capacity Analysis for Vehicular Ad Hoc Networks

XINXIN HE[1], WEISEN SHI[2], AND TAO LUO[3], (Senior Member, IEEE)
[1]Beijing Key Laboratory of Network System Architecture and Convergence, Beijing University of Posts and Telecommunications, Beijing 100876, China
[2]Department of Electrical and Computer Engineering, University of Waterloo, Waterloo, ON N2L 3G1, Canada
[3]Beijing Laboratory of Advanced Information Network, Beijing University of Posts and Telecommunications, Beijing 100876, China

Corresponding author: Xinxin He (hxx_9000@bupt.edu.cn)

This work was supported in part by the National Natural Science Foundation of China under Grant 61571065 and in part by the China Postdoctoral Science Foundation under Grant 2017M620695.

ABSTRACT Traditional studies focused on the transmission capacity of vehicular ad hoc network (VANET) contains two deficiencies: the lack of a realistic model mimicking the behaviors of vehicles and the failure to consider the impacts from enhanced distributed channel access (EDCA) mechanisms applied by IEEE 802.11p. In this paper, the car-following model is introduced to describe the distribution of vehicles, and an EDCA-based linear VANET model is analyzed. Compared to previous works, a tighter transmission capacity upper bound in a large-scale fading environment is calculated. Furthermore, under Rayleigh fading channels, an elementary expression of transmission capacity fitting a sparse vehicles scenario and an upper bound of transmission capacity applicable to a dense scenario are obtained. In conclusion, the transmission capacity of a linear VANET is illustrated by the elementary expression in a sparse vehicles scenario and the upper bound in a dense vehicles scenario. The simulation results are well constrained by the proposed theoretical expression and upper bound.

INDEX TERMS Car-following model, EDCA, transmission capacity, VANET.

I. INTRODUCTION

Based on Gupta and Kumar's theoretical bound on the capacity of ad hoc networks [1], Weber and Andrews [2] developed the concept and expression of transmission capacity (TC) in ad hoc networks. Regarding vehicular ad hoc networks (VANET) as one kind of ad hoc network with mobile nodes (vehicles), some researchers used TC as the indicator of VANET capacity [3]–[5]. However, not only did the researchers introduce the theory of TC, they also inherited the network topology and MAC layer mechanisms of ad hoc networks. Since vehicles travel along roads, the 2-dimensional Poisson point process (2-D PPP), which is the most common topology model used in ad hoc networks, is inappropriate to describe their behaviors. However, the medium access control (MAC) layer mechanisms investigated by those studies, such as ALOHA or time division multiple access (TDMA), are too basic to model the enhanced distributed channel access (EDCA) mechanism in IEEE 802.11p [6], [7], which is accepted as the standard in VANET communication. With these two defects in modeling the VANET topology and the EDCA mechanism, it is necessary to introduce new models into VANET research.

Some researchers proposed grid models [8], [9] and linear road models [10], [11] to estimate more realistic capacities for VANET. In [8] and [9], Pishro-Nik *et al.* and Nekoui *et al.* showed that the asymptotic boundaries of VANET's TC in a downtown grid scenario are $\Omega(1/n)$ and $\Omega(1/n \ln n)$ when vehicles are uniformly and exponentially distributed along roads, respectively. Jacquet and Muhlethaler [10] investigated the linear VANET, in which vehicular networks are constructed on a 1-dimensional long road. They proposed both upper and lower bounds of TC in a linear VANET but ignored the impacts of interference. In [11], Giang *et al.* proposed their estimation of the TC upper bound in a linear VANET and studied the impacts of the carrier sense multiple access with collision avoidance (CSMA/CA) mechanism. Nevertheless, for each transmitter in [11], they only considered the interference from the two adjacent simultaneous transmitters. They also introduced an estimated constant to fit the calculation of the upper bound. These two defects make the upper bound calculation mostly invalid, especially in a dense vehicles scenario.

Inspired by [11], in this paper, we built a 1-dimensional linear VANET model considering the impacts of the EDCA mechanism, which has similar impacts as CSMA/CA when all EDCA data packets hold the same priority [12]. The distribution of vehicles follows the car-following model, which is a widely accepted model to describe vehicle behavior in transportation research [13]. Considering the interference from all possible interfering transmitters, a tighter TC upper bound than that in [11] is proposed. To obtain more realistic conclusions, performances of the linear VANET model in a Rayleigh fading environment are tested. In a Rayleigh fading environment, a TC upper bound for the dense vehicles scenario is given. However, this upper bound is not high enough for a sparse vehicles scenario. To estimate the TC in a sparse vehicles scenario, the assumption in [11] that each transmitter is only disrupted by its two adjacent simultaneous transmitters is accepted, then an elementary expression of TC that fits the simulation results well in sparse vehicles scenarios is deduced. As a result, the TC of a linear VANET is depicted by an elementary expression in a sparse vehicles scenario and with an upper bound in a dense vehicles scenario. Compared with [11], this work provides a more valid upper bound of TC and develops new results in a Rayleigh fading environment.

The rest of the paper is organized as follows. The theoretical model of a linear VANET is introduced in Section II. The deduction and conclusions of our TC upper bound are shown in Section III. The elementary expression and upper bound of TC under Rayleigh fading channels are analyzed in Section IV. Finally, the paper is concluded in Section V.

II. MODEL OF THE LINEAR VANET

A. CAR-FOLLOWING MODEL

The moving pattern of vehicles in the linear VANET is described as the classic car-following model, which claims that the mean distance X between any two adjacent vehicles on a linear road follows a log-normal distribution parameterized by μ and σ [13]:

$$D_{logn}(x, \mu, \sigma) = \frac{1}{\sqrt{2\pi}\sigma x} \exp\left(\frac{-(\ln x - \mu)^2}{2\sigma^2}\right), \tag{1}$$

The car-following model is deduced through experimental data and widely applied in transportation research. Compared with the 2-D PPP, this model represents more realistic behaviors of vehicles in a linear VANET.

B. MODEL OF EDCA's IMPACTS

According to the EDCA mechanism, application messages are categorized into four queues with different priorities. Each queue fulfills a classical CSMA/CA mechanism with specific parameters [12]. The main purpose of the EDCA mechanism is to ensure the different priorities of different services, but researchers studying TC used to set all data-packets into the same priority to simplify the research. Thus, the task of modeling EDCA turns into modeling CSMA/CA [12].

In a CSMA/CA mechanism, transmitters sense the channel before transmitting, and decide whether to transmit or postpone according to channel states, idle or occupied. There are there clear channel assessment (CCA) modes deciding the channel states. This work applies CCA Mode 1, in which the channel state would be busy as long as the total power of the interferences is higher than the threshold θ. Since the power of interferences is mainly determined by the distances between the transmitter and its interfering sources, the CCA mechanism in CSMA/CA limits the minimal distance between two adjacent simultaneous transmitters and the maximal number of simultaneous transmitters over a dedicated space.

C. LINEAR VANET MODEL

Our theoretical model of a linear VANET is shown in Fig. 1. All transmitting vehicles, share the same transmitting data rate R and the same transmitting power Pt. Each transmitter holds a maximal effective transmission radius D, which is approximately 500 meters. Transmitters are distributed along a linear road with a length L and a width W.

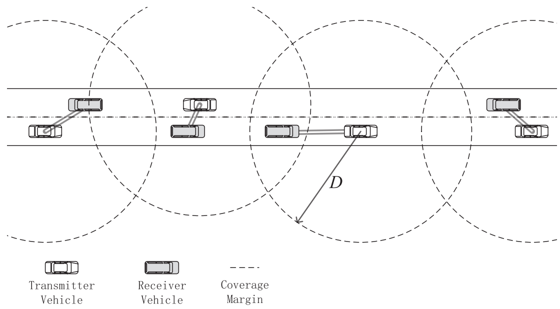

FIGURE 1. Basic illustration of theoretical model.

Without loss of generality, assuming $L \gg D$ and $D \gg W$, the road is abstracted as a 1-dimensional infinite line. Therefore, the signal coverage of one transmitter is illustrated as a $2D$-length segment with the transmitter at the midpoint.

The path-loss function $P_L(.)$ is defined as a Friis transmission equation:

$$P_L(d) = \begin{cases} P_t G_t G_r \left(\frac{\lambda}{4\pi d}\right)^{\alpha} = \frac{A}{d^{\alpha}} & 1 < d \le D \\ 0 & d > D, \end{cases} \tag{2}$$

where G_t and G_r are gains of the transmitting and receiving antennas respectively. λ is the wavelength. P_t is transmission power.$d$denotes the distance between one pair of transmitter and receiver. The exponent α is typically chosen between 2 to 5. Since G_t, G_r, λ, P_t and α are constants here, the constant A is introduced instead of the multiplication of all the constants in (2).

III. UPPER BOUND OF TRANSMISSION CAPACITY IN EDCA-BASED LINEAR VANET

A. UPPER BOUND OF TC

As aforementioned, the maximal number of simultaneous transmitters over a dedicated space is constrained due to EDCA's impacts. It is possible to use this limitation to calculate the maximal density of simultaneous transmitters on the linear VANET, which is a key intermediate result in estimating the upper bound of TC. Considering an extreme case where no additional simultaneous transmitters could be added, the distribution of simultaneous transmitters has two special attributes:

- All transmitters are located in positions where the total power of interferences suffered by each of them is equal to or less than the threshold θ. This attribute guarantees the valid and simultaneous transmission of all transmitters.
- The total power of interferences in any position between two adjacent transmitters is higher than θ. Since a transmitter would postpone its transmission as long as the total interference power is higher than θ, this attribute guarantees no new transmitter could be added between any two existing adjacent transmitters, and it is impossible for any existing transmitters to find a more desirable position or suffer less interference than θ.

Obviously, under this specific distribution of transmitters, the maximal number of simultaneous transmitters over the linear road would be approached.

Adopting the linear VANET model and taking all possible interfering transmitters into account, one can finally prove that a uniform distribution meets both attributes.

Lemma 1: In the extreme case where the maximal density of simultaneous transmitters is reached, all simultaneous transmitters are uniformly distributed over the linear road with the same minimal distance between each other.

Proof: Assume the uniform distribution in Lemma 1 is achieved. The total power of interferences, denoted by I_c, suffered by each simultaneous transmitter, is expressed as equation (3), which just equals θ:

$$I_c = A\sum_{n=1}^{K_m}\frac{2}{(nD_{min})^{\alpha}} = \theta, \tag{3}$$

where K_m denotes the maximal possible number of other simultaneous transmitters within current transmitter's one-side signal coverage D, and D_{min} denotes the minimal distance between two adjacent transmitters. The total number of simultaneous transmitters within the signal coverage of the current transmitter is $2K_m + 1$, including the current transmitter itself.

For a randomly chosen position i between any two adjacent simultaneous transmitters, the offset between i and its right-side transmitter is $\Delta(0 \leq \Delta \leq \mathrm{D}/\mathrm{K_m})$. Therefore, the total interference energy in position i is:

$$I_i = A\sum_{n=1}^{K_m}\left[\frac{1}{(nD_{min}+\Delta)^{\alpha}} + \frac{1}{(nD_{min}-\Delta)^{\alpha}}\right]. \tag{4}$$

Comparing (3) and (4) when setting nD_{min} as a_n, equations (3) and (4) can be rewritten as:

$$I_c = A\sum_{n=1}^{K_m}\frac{2}{a_n^{\alpha}}, \tag{5}$$

$$I_i = A\sum_{n=1}^{K_m}\left[\frac{1}{(a_n+\Delta)^{\alpha}} + \frac{1}{(a_n-\Delta)^{\alpha}}\right], \tag{6}$$

Deducing from the attributes of convex functions, it is easy to prove that:

$$\frac{1}{(a_n+\Delta)^{\alpha}} + \frac{1}{(a_n-\Delta)^{\alpha}} - \frac{2}{a_n^{\alpha}} \geq 0 \quad (\alpha \geq 2), \tag{7}$$

According to equation (7), one can conclude that I_i is always greater than I_c, which is equal to θ. Since position i denotes any position between two adjacent transmitters, it is safe to say that under uniform distribution, the total interference energy in any position not occupied by existing simultaneous transmitters is greater than the threshold θ. Therefore, the maximal density of simultaneous transmitters would be approached when all simultaneous transmitters follow a uniform distribution with the minimal inter-transmitter distance D_{min}. Lemma 1 is proved.

Deducing from Lemma 1, equation (3) could be revised as:

$$\frac{\theta D_{min}^{\alpha}}{2A} = \sum_{n=1}^{K_m}\frac{1}{n^{\alpha}}. \tag{8}$$

Since equation (8) contains a general harmonic number that is difficult to calculate, we use the attributes of convex functions (See equation (7) in the proof of Lemma 1) again to transform equation (8) into a closed form:

$$\frac{\theta D_{min}^{\alpha}}{2A} \geq 1 + \frac{2^{\alpha}\left(K_m-1\right)}{\left(K_m+2\right)^{\alpha}}, \tag{9-1}$$

$$D_{min} \geq \left[\frac{2A}{\theta} + \frac{2^{\alpha+1}\left(K_m-1\right)A}{\theta\left(K_m+2\right)^{\alpha}}\right]^{1/\alpha} \tag{9-2}$$

$$s.t.\ \begin{cases} K_m D_{min} \leq D \\ \left(K_m+1\right)D_{min} > D, \end{cases} \tag{9-3}$$

Every K_m has a corresponding minimal value of D_{min} when the equal sign is held in (9-2). However, due to the constraint in (9-3), only one specific pair of K_m and $D_{min}$is valid in each specific scenario.

The expression of transmission capacity C_T is defined as:

$$C_T = \rho_m\left(1-\varepsilon\right)R, \tag{10}$$

where ε is outage probability, ρ_m is the density of simultaneous transmitters, and R is the transmission data rate [2]. Since all simultaneous transmitters are uniformly distributed over the linear road, the maximal ρ_m is equal to $1/D_{min}$. Hence, when keeping R and ε as constant, the upper bound of TC in the linear VANET becomes:

$$C_{up} = \frac{(1-\varepsilon)R}{D_{min}}, \tag{11-1}$$

$$C_{up} = \frac{(1-\varepsilon)R}{\left[\frac{2A}{\theta} + \frac{2^{\alpha+1}(K_m-1)A}{\theta(K_m+2)^{\alpha}}\right]^{1/\alpha}}. \tag{11-2}$$

This upper bound limits the maximal possible value of transmission capacity for a dedicated linear VANET.

B. SIMULATION RESULTS

We build a linear VANET environment with Matlab to validate the upper bound. All parameters are shown in Table 1. To compare with the upper bound in [11], we accept the assumption that ε equals 0 when the linear VANET reaches its TC upper bound.

TABLE 1. Simulation parameters.

Simulation Parameter	Numerical Value
IEEE 802.11std	802.11p
CCA mode	CCA mode 1
Carrier Wavelength λ	0.051 m
Packet Length	2048 byte
Slot-time	20 μs
[CW_{min} , CW_{max}]	[140 μs, 300 μs]
Arbitration Inter-Frame Space (AIFS)	50 μs
Short Inter-frame Space (SIFS)	10 μs
Transmission Power P_t	33 dBm
Transmission Gain G_t	34 dBm
Receiving Gain G_r	33 dBm
CCA Threshold θ	-50 dBm
Exponent α	2
Outage Probability ε	0
Transmission Data Rate R	2 Mbps
Effective Transmission Radium D	500 m
Road Length L	4 km
Duration of Simulation t_s	3 seconds

Fig. 2 shows the simulation results of average transmission capacity. Through solving equations (9-2) and (9-3) with the parameters in Table 1, we conclude that D_{min} in the simulation environment equals 213.31 m, and the upper bound of TC C_{up} is 9376.03 bps/m, which is plotted as the triangle-dotted line in Fig. 2. The square-dotted line represents the results of [11]. The solid curve with the error-bar and the circle-dotted curve depict the average and maximal simulated values of TC, respectively, for 20 simulations. Obviously, the upper bound in [11] constrains the average TC (dash-dotted curve) better,

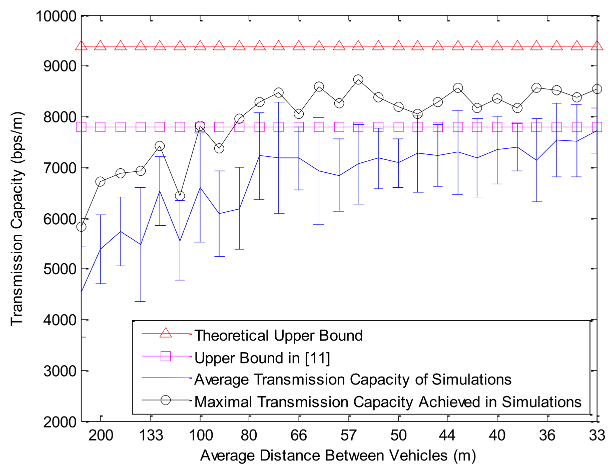

FIGURE 2. Average transmission capacity and upper bound.

but many of the simulation results, especially the maximal values in the circle-dotted curve, still exceed the bound. Though not tight enough to constrain the average value curve, the proposed upper bound does constrain the maximal value of all simulations well with no exceeding results.

The reason for the different performances of the two upper bounds is model difference. In paper [11], Giang *et al.* only consider the interference of two adjacent simultaneous transmitters and multiply their result with a constant estimated from simulations. Therefore, their upper bound turns out to be a constraint for the average value of TC exactly. While in our model, almost all possible interferences are included, without any estimated constant. For this reason, our upper bound is a better constraint for the maximal value of TC rather than the average one.

We also investigate instantaneous transmission. The circle-dotted curves in Fig. 3 and Fig. 4 depict the maximal instantaneous TC and maximal instantaneous density of simultaneous transmitters of the 20 simulations.

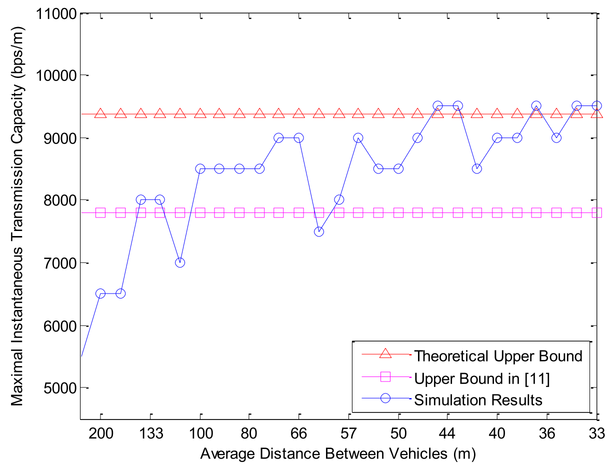

FIGURE 3. Maximal instantaneous transmission capacity and upper bound.

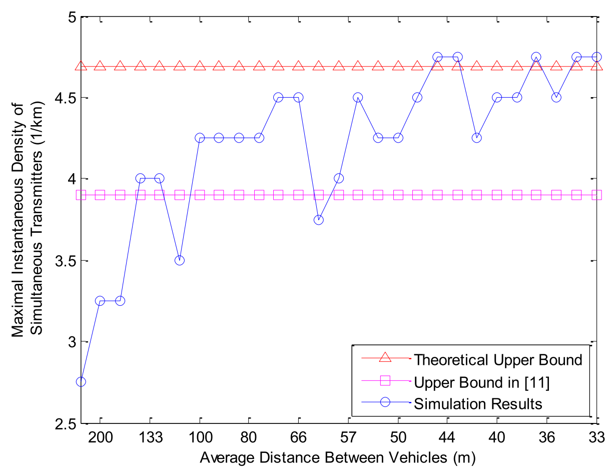

FIGURE 4. Average transmission capacity and upper bound.

In this case, the upper bounds of [11] (square-dotted lines) are no longer valid, but our upper bounds (triangle-dotted lines in both figures) constrain the simulation results well.

Note that both curves of the simulation results in the two figures slightly exceed our upper bound. This is caused by the impacts from less interfered transmitters located near the two endpoints of the 4 km road. Since the theoretical upper bound is deduced under an infinite road scenario where all transmitters are interfered by other transmitters from both left and right sides, the transmitters near the endpoints of the 4 km simulated road environment would lack some interference from one side. In the simulation scenario, the upper bound of the maximal number of simultaneous transmitters over the whole road is 4 km/D_{min}, which equals 18.75, while the maximal simulation result is 19. Therefore, the transmitters near the endpoints only cause a small exceeding of the upper bound, and its impacts will decrease with the increasing of road length.

According to all the simulation results, our theoretical upper bound provides a better constraint of TC in a linear VANET.

IV. TRAMSMISSION CAPACITY OF LINEAR VANET UNDER RAYLEIGH FADING CHANNELS

A. ELEMENTARY EXPRESSION OF TC UNDER RAYLEIGH FADING CHANNELS

To analyze the TC of a linear VANET in a more realistic environment, we extend the conclusion in Section III by considering the impacts of Rayleigh fading. Then, equation (2) is revised as:

$$P_L\left(d\right) = H_0 A d^{-\alpha}, \tag{12}$$

where H_0 is the Rayleigh fading factor, which is a random variable whose PDF is the exponential distribution with parameter τ:

$$h_{Ray}\left(x\right) = \tau e^{-\tau x} \quad (x \geq 0), \tag{13}$$

where $\tau = 1/2\sigma^2$ [14]. σ is the variance of the normal distribution, which forms the Rayleigh distribution depicting the Rayleigh fading.

Due to fading, the outage probability ε is no longer constant, and the distance between transmitter and receiver affects the TC. With variable ε impacted by Rayleigh fading, the distribution of vehicles defined by the car-following model, and all possible interfering sources taken into account, the calculation of TC becomes a difficult task, and the mathematical expression of the conclusion would be complex, even unsolvable. To simplify the calculation and deduce an elementary expression of TC, we accept the assumption in [11] that each transmitter is only interfered with by its two adjacent simultaneous transmitters. Fig. 5 shows the new linear VANET model for calculating an elementary expression of TC.

In Fig. 5, T is the current transmitter and R is its corresponding receiver. T_L and T_R are the left and right side interference transmitters, respectively. I_{RL}, I_{RR}, I_{TL}, I_{TR} indicate the power of interference between each vehicle, noticing that the receiver is also affected by interference. S_{TR} is the power

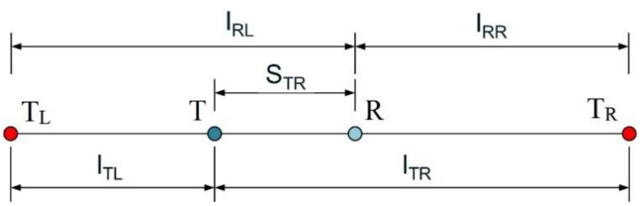

FIGURE 5. Linear VANET model for calculating elementary expression of TC.

of the transmitted signal. The distances between any adjacent vehicles in Fig. 5 follow the car-following model.

As equation (10) shows, the TC of a network is determined by two main parameters: the density of simultaneous transmitters and the outage probability. In the new linear VANET model, the density of simultaneous transmitters ρ_{logn} is defined as:

$$\frac{1}{\rho_{logn}} = \frac{E\left(X\right) + E\left(X_2\right)}{2} = \frac{e^{\mu+\sigma^2/2} + e^{\mu_2+\sigma_2^2/2}}{2}, \tag{14}$$

where X represents the distance between T_L and T, which follows the log-normal distribution defined in equation (1). X_2 is the distance between T_R to T. According to the Fenton-Wilkinson method [15], X_2 follows a log-normal distribution parameterized by μ_2 and σ_2.

$$\mu_2 = ln\left(2e^{\mu}\right) + \left(\sigma^2 - \sigma_2^2\right)/2, \tag{15}$$

$$\sigma_2 = ln\left(\frac{e^{\sigma^2} - 1}{2} + 1\right). \tag{16}$$

However, because of the impacts of Rayleigh fading, ρ_{logn} must multiply a successful transmission probability Pr_t when it is used to calculate TC. The deduction of Pr_t is a hard process, and the expression of Pr_t, as far as we know, remains in a complex form:

$$\begin{aligned} Pr_t\left(z < \theta\right) = \int_0^{\theta}\int_0^{z} &\left\{D_{logn}\left[i_L, ln\left(H_0A\right) - \alpha\mu, \alpha^2\sigma^2\right]\right. \\ &\times D_{logn}[z - i_L, ln\left(H_0A\right) \\ &\left. - \alpha\mu_2, \alpha^2\sigma_2^2]\right\} di_L dz. \end{aligned} \tag{17}$$

where $D_{logn}(.)$ is defined in equation (1), i_L represents I_{TL} and z-i_L represents I_{TR}. Using the attributes of log-normal distribution, it is easy to prove that when $X \sim D_{logn}(x, \mu, \sigma)$, then $i_L \sim D_{logn}[i_L, ln(H_{0A}) - a\mu, a^2\sigma^2]$.

The analyzing of receivers mainly concentrates on the outage probability ε_{logn}:

$$\varepsilon_{logn} = Pr\left(\frac{I_d}{I_x + I_{x_2}} \leq \beta\right). \tag{18}$$

In equation (18), I_d, I_x and I_{x_2} indicate S_{TR}, I_{RR} and I_{RL} respectively. β is the threshold of SIR according to the definition of outage probability. Similar to equation (17), equation (18) also contains tough calculations of different random variables. To our best knowledge, no simple form of (18) is found.

Despite being filled with complex mathematical calculations, a general form of the elementary expression of TC in the linear VANET is available, as shown in equation (19):

$$C = Pr_t(\theta)\,\rho_{logn}\left(1-\varepsilon_{logn}\right)R. \tag{19}$$

B. UPPER BOUND OF TC UNDER RAYLEIGH FADING CHANNELS

The elementary expression of TC depends on the linear VANET model, which considers adjacent transmitters' interference only. This defect decreases the expression's accuracy in dense vehicle scenarios. To compensate for this defect, we extend the conclusion in Section III to calculate the upper bound of TC under Rayleigh fading channels.

Combining equation (3) and equation (12), the expression of I_c is revised as:

$$I_c = A\sum_{i=1}^{M}\frac{H_i}{d_i^{\alpha}} \le \theta \quad (d_i < D), \tag{20}$$

where d_i is the distance between transmitter and its ith interfering source, and H_i is the Rayleigh fading factor of this path. Since H_i is a random variable, it is impossible to obtain an invariant D_{min} through equation (20). Therefore, the D_{min} in Section III has to be revised as D_{min_A}, which is an average or expected value of a large number of d_i. Through calculating the expectation of H_i, we have the expression of D_{min_A}:

$$E\left(2A\sum_{i=1}^{K}\frac{H_i}{\left(iD_{\min\_A}\right)^{\alpha}}\right) \le \theta, \tag{20-1}$$

$$2AE\left(H_i\right)\frac{\left(1+2^{\alpha}\left(K_m-1\right)/\left(K_m+2\right)^{\alpha}\right)}{D_{min\_A}^{\alpha}} \le \theta, \tag{20-2}$$

$$2A\frac{\left(1+2^{\alpha}\left(K_m-1\right)/\left(K_m+2\right)^{\alpha}\right)}{D_{min\_A}^{\alpha}} \times\left(\int_0^{+\infty}\tau exp\left(-\tau h\right)dh\right) \le \theta, \tag{20-3}$$

$$D_{min\_A} \ge \left[\frac{2A\tau}{\theta}+\frac{2^{\alpha+1}\left(K_m-1\right)A\tau}{\theta\left(K_m+2\right)^{\alpha}}\right]^{1/\alpha}. \tag{20-4}$$

The transformation from (20-1) to (20-2) utilizes the same convex function attribute as in Section III.

In a Rayleigh fading environment, outage probability should not be treated as a constant. By defining d_{tr} as the distance between a transmitter and its corresponding receiver, the outage probability for the receiver is (21), as shown at the bottom of this page.

Using the same transformation method as in [16], equation (21) can be rewritten as (22), shown at the bottom of this page.

Note that in $F(.)$, I_d and I_a contain similar general harmonic numbers in Section III. After utilizing the attribute of convex function, the final expression of ε_R is:

$$\varepsilon_R = 1-\left\{\frac{\tau}{\frac{2^{\alpha+1}\tau\beta d_{tr}^{\alpha}}{\left[(K_m+1)D_{\substack{\min\\A}}-2d_{tr}\right]^{\alpha}}+\tau}\right\}^{\frac{K_m}{2}} \times\left\{\frac{\tau}{\frac{2^{\alpha+1}\tau\beta d_{tr}^{\alpha}}{\left[(K_m+1)D_{\substack{\min\\A}}+2d_{tr}\right]^{\alpha}}+\tau}\right\}^{\frac{K_m}{2}}. \tag{23}$$

Substituting D_{min_A} and ε_R for D_{min} and ε in equation (11-1), the upper bound of TC under Rayleigh fading channels is:

$$C_{up\_Ray} = \frac{(1-\varepsilon_R)R}{D_{\min\_A}}. \tag{24}$$

C. SIMULATION RESULTS AND ANALYSIS

Based on the simulation environment in Section III, we substitute Rayleigh fading channels for the path-loss fading defined by equation (2). To simplify the simulation, we set τ equal to 1 and d_{tr} equal to 50 m, while the threshold β is 5. Other parameters are the same as in Table 1.

Fig. 6 shows the performance of the elementary expression. The solid curve with error bars depicts the average simulated result of TC under Rayleigh fading channels for 20 simulations. The circle-dotted curve is the numerical result of equation (19), which is the elementary expression of TC. The square-dotted line is the upper bound in [11]. It is obvious that the elementary expression fits the simulation results well in a sparse vehicles scenario in which the average distance

$$\varepsilon_R = Pr\left\{\frac{AH_0 d_{tr}^{-\alpha}}{A\sum_{i=0}^{K_m}H_i\left(iD_{min}-d\right)^{-\alpha}+A\sum_{i=0}^{K_m}H_i\left(iD_{min}+d\right)^{-\alpha}} \le \beta\right\} \tag{21}$$

$$\begin{aligned}\varepsilon_R &= Pr\left\{\frac{AH_0 d_{tr}^{-\alpha}}{A\sum_{i=0}^{K_m}H_i\left(iD_{min}-d\right)^{-\alpha}+A\sum_{i=0}^{K_m}H_i\left(iD_{min}+d\right)^{-\alpha}} \le \beta\right\}\\ &= Pr\left\{H_0 \le \beta d_{tr}^{\alpha}\left[\sum_{i=0}^{K_m}H_i\left(iD_{min}-d\right)^{-\alpha}+\sum_{i=0}^{K_m}H_i\left(iD_{min}+d\right)^{-\alpha}\right]\right\}\\ &= 1-E\left[\exp\left(-\tau\beta d_{tr}^{\alpha}\left(I_d+I_a\right)\right)\right]\\ &= 1-F\left(\tau\beta d_{tr}^{\alpha}\left(I_d+I_a\right)\right).\end{aligned} \tag{22}$$

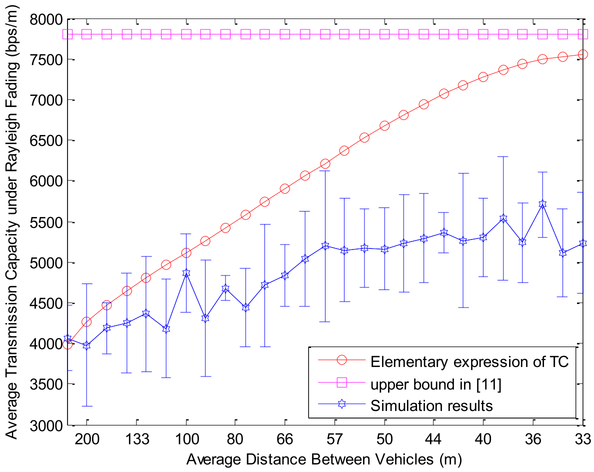

FIGURE 6. **Elementary expression of TC fits simulation results in sparse vehicles scenario.**

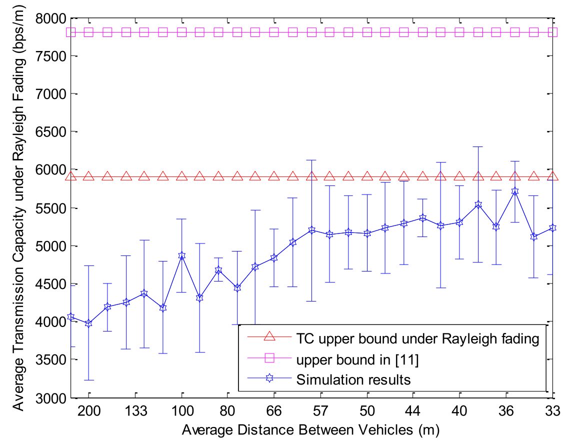

FIGURE 7. **Upper bound of TC fits simulation results in dense vehicles scenario.**

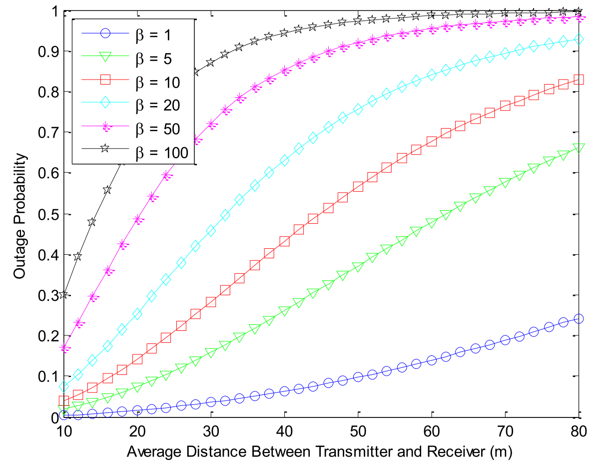

FIGURE 8. **Outage probability influenced by d_{tr} and β.**

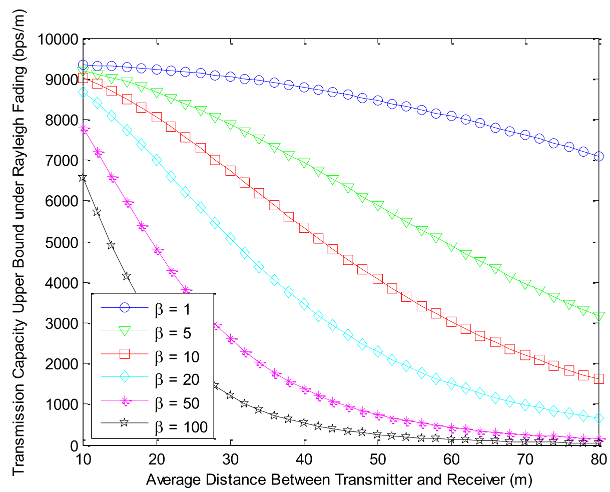

FIGURE 9. **Upper bound of TC influenced by d_{tr} and β.**

between adjacent vehicles (regardless of whether they are transmitters or receivers) is more than 50 meters. While for the dense vehicles scenario, where average distance between adjacent vehicles is less than 50 meters, the elementary expression does not fit the simulation results anymore, but approaches [11]'s upper bound. This inaccuracy is caused by the assumption that each transmitter is only interfered by its two adjacent simultaneous transmitters when we deduce the elementary expression. Since both the elementary expression and [11]'s upper bound are based on similar models without the consideration of all possible interferences, in the situation where the total interference is not determined by only two adjacent transmitters, such as in a dense vehicles scenario, the models would likely lose their accuracy.

The reason we only choose the adjacent two transmitters' interference is the calculation complexity. With variable ε impacted by Rayleigh fading, as well as the log-normal distribution of vehicles defined by the car-following model, taking all possible interfering sources into account would make the mathematical analyses and calculation of the elementary expression to be complex, even unsolvable. One way to improve it is leveraging more mathematical tools to approximate or solve the complex expression considering all possible interference, which can be the future research direction of us.

In the dense traffic scenario, the upper bound defined by equation (24) estimates the TC of a linear VANET. In Fig. 7, the triangle-dotted line depicts the upper bound, and it fits the simulation results curve well in a dense vehicles scenario.

When analyzing the TC of a linear VANET under Rayleigh fading channels, d_{tr} and β are newly involved essential parameters. Fig. 8 and Fig. 9 illustrate their impact on the outage probability and the TC upper bound, respectively. From the two figures, we infer that when $\beta \in [5, 50]$, changing d_{tr} might cause significant variations of outage probability and the TC.

Combining the analysis results of Fig. 6 and Fig. 7, we conclude that for the linear VANET under Rayleigh fading channels, the elementary expression fits the estimation of TC in a sparse vehicles scenario, while the upper bound of TC fits in a dense vehicles scenario. Through depicting the minimal value between C and C_{up_Ray}, a combined expression of TC is shown as the circle-dotted curve in Fig. 10. In a

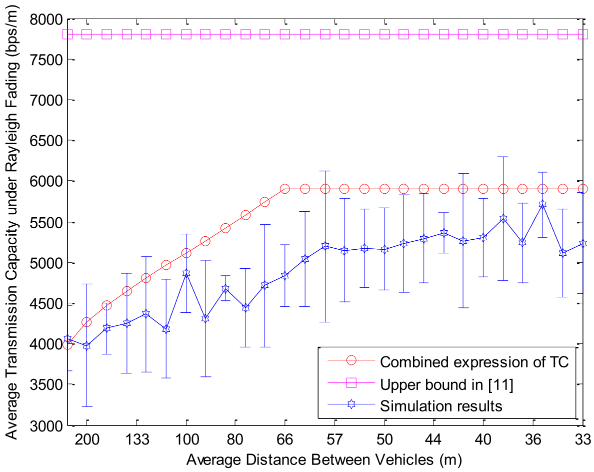

FIGURE 10. Combined expression of TC fits simulation results.

sparse vehicles scenario, the curve is formed by the values calculated from the elementary expression of TC, while in the dense trafficscenario, the curve is equal to C_{up_Ray}. Through calculating the intersecting point of curve C and C_{up_Ray}, the threshold density dividing the sparse and dense vehicles scenarios can be obtained, which just equals the x-coordinate of the intersection point.

Generally speaking, the large scale fading analyses in this paper are preliminary works to propose a more valid upper bound than [11], while the Rayleigh fading analyses are the extensions of the preliminary works to investigate the upper bound and elementary expression of TC in a more realistic scenario.

V. CONCLUSION

In this work, the TC of the EDCA-based linear VANET in a large-scale fading environment and a Rayleigh fading environment are analyzed. The car-following model is introduced to imitate a realistic vehicular environment. Compared with the previous work [11], a tighter TC upper bound in the large-scale fading environment is proposed. In the Rayleigh fading environment, an elementary expression of TC applying to a sparse traffic scenario, and a TC upper bound applying to a dense traffic scenario are deduced. As a result, the TC of a linear VANET under Rayleigh fading channels is calculated by the elementary expression of TC in a sparse traffic scenario, and the upper bound C_{up_Ray} in a dense traffic scenario.

For next step, the elementary expression of TC in Section IV should be simplified. In addition, some fading models applying to a vehicular environment, such as Weibull fading [17], should be considered in future work.

REFERENCES

[1] P. Gupta and P. R. Kumar, "The capacity of wireless networks," *IEEE Trans. Inf. Theory*, vol. 46, no. 2, pp. 388–404, Mar. 2000.

[2] S. P. Weber and J. G. Andrews, "Transmission capacity of wireless networks," *Found. Trends Netw.*, vol. 5, nos. 2–3, pp. 109–281, 2012.

[3] M. Franceschetti, O. Dousse, D. N. C. Tse, and P. Thiran, "Closing the gap in the capacity of wireless networks via percolation theory," *IEEE Trans. Inf. Theory*, vol. 53, no. 3, pp. 1009–1018, Mar. 2007.

[4] V. P. Mhatre, C. P. Rosenberg, and R. R. Mazumdar, "On the capacity of ad hoc networks under random packet losses," *IEEE Trans. Inf. Theory*, vol. 55, no. 6, pp. 2494–2498, Jun. 2009.

[5] S. P. Weber, X. Yang, J. G. Andrews, and G. de Veciana, "Transmission capacity of wireless ad hoc networks with outage constraints," *IEEE Trans. Inf. Theory*, vol. 51, no. 12, pp. 4091–4102, Dec. 2005.

[6] H. Hartenstein and K. P. Laberteaux, *VANET: Vehicular Applications and Inter-Networking Technologies*. Chichester, U.K.: Wiley, 2010.

[7] *Standard Specification for Telecommunications and Information Exchange Between Roadside and Vehicle Systems—5 GHz Band Dedicated Short Range Communications (DSRC) Medium Access Control (MAC) and Physical Layer (PHY) Specifications*, Standard ASTM E2213-03, Jul. 2003.

[8] H. Pishro-Nik, A. Ganz, and D. Ni, "The capacity of vehicular ad hoc networks," in *Proc. 45th Annu. Allerton Conf. Commun., Control Comput.*, Sep. 2007, pp. 267–272.

[9] M. Nekoui, A. Eslami, and H. Pishro-Nik, "Scaling laws for distance limited communications in vehicular ad hoc networks," in *Proc. IEEE Int. Conf. Commun.*, May 2008, pp. 2253–2257.

[10] P. Jacquet and P. Muhlethaler, "Mean number of transmissions with CSMA in a linear network," in *Proc. IEEE Veh. Technol. Conf. Fall*, Sep. 2010, pp. 1–5.

[11] A. T. Giang, A. Busson, D. Gruyer, and A. Lambert, "A packing model to estimate VANET capacity," in *Proc. IEEE Wireless Commun. Mobile Comput. Conf.*, Aug. 2012, pp. 1119–1124.

[12] J. R. Gallardo, D. Makrakis, and H. T. Mouftah, "Performance analysis of the EDCA medium access mechanism over the control channel of an IEEE 802.11p wave vehicular network," in *Proc. IEEE Int. Conf. Commun.*, Jun. 2009, pp. 1–6.

[13] M. Brackstone and M. McDonald,"Car-following: A historical review," *Transp. Res. F, Traffic Psychol. Behav.*, vol. 2, no. 4, pp. 181–196, 1999.

[14] T. S. Rappaport, *Wireless Communications: Principles and Practice*. Upper Saddle River, NJ, USA: Prentice-Hall, 2001.

[15] M. Ni, J. Pan, L. Cai, J. Yu, H. Wu, and Z. Zhong, "Interference-based capacity analysis for vehicular ad hoc networks," *IEEE Commun. Lett.*, vol. 19, no. 4, pp. 621–624, Apr. 2015.

[16] X. He, W. Shi, and T. Luo, "Broadcast transmission capacity of VANETs with secrecy outage constraints under multiple frequency bands," in *Proc. IEEE Veh. Technol. Conf.*, May 2015, pp. 1–5.

[17] I. Sen and D. W. Matolak, "Vehicle–vehicle channel models for the 5-GHz band," *IEEE Trans. Intell. Transp. Syst.*, vol. 9, no. 2, pp. 235–245, Jun. 2008.

[18] W. Shi, X. He, T. Luo, and L. Ding, "Estimating the upper bound of transmission capacity in linear VANET," in *Proc. IEEE Int. Wireless Commun. Mobile Comput. Conf. (IWCMC)*, Aug. 2015, pp. 1347–1351.

XINXIN HE received the B.S. degree from the Nanjing University of Posts and Telecommunications in 2009 and the M.S. degree from the Kunming University of Science and Technology in 2013. She is currently pursuing the Ph.D. degree with the School of Information and Communication Engineering, Beijing University of Posts and Telecommunications. Her research interests include VANET and cognitive radio networks.

WEISEN SHI received the B.S degree from Tianjin University in 2013 and the M.S. degree from the Beijing University of Posts and Telecommunications in 2016. He is currently pursuing the Ph.D. degree with the Department of Electrical and Computer Engineering, University of Waterloo. His research interests include the Internet of vehicles and software-defined networks.

TAO LUO (M'09–SM'15) is currently a Professor with the Beijing Key Laboratory of Network System Architecture and Convergence, Beijing University of Posts and Telecommunications, China. His research interests include mobile communication, cognitive radio networks, Internet of Vehicles, and machine learning.